# Optical Engineering

OpticalEngineering.SPIEDigitalLibrary.org

# High efficiency mid-infrared interband cascade LEDs grown on low absorbing substrates emitting >5 mW of output power

Nicolas Schäfer
Julian Scheuermann
Robert Weih
Johannes Koeth
Sven Höfling

SPIE.

# High efficiency mid-infrared interband cascade LEDs grown on low absorbing substrates emitting >5 mW of output power

**Nicolas Schäfer,[a,*] Julian Scheuermann,[a] Robert Weih,[a] Johannes Koeth,[a] and Sven Höfling[b,c]**
[a]nanoplus Nanosystems and Technologies GmbH, Gerbrunn, Germany
[b]Universität Würzburg, Technische Physik and Wilhelm Conrad Röntgen Research Center for Complex Material Systems, Würzburg, Germany
[c]University of St. Andrews, Scottish Universities Physics Alliance, School of Physics and Astronomy, St. Andrews, United Kingdom

**Abstract.** We present interband cascade light-emitting devices with incoherent and broadband light emission peaked at a wavelength of around 3.7 $\mu$m. The substrate-side-emitting devices display higher wall plug efficiencies and maximum output powers than any earlier mid-infrared LEDs operating in continuous wave at room temperature. To reduce absorption losses, the epitaxial structures were grown on low doped (low absorbing) GaSb substrates. The nine active stages were positioned in different configurations to investigate the impact of constructive or destructive interference when reflected from the epitaxial-side metallization of the flip-chip mounted devices. A comparison shows improved electrical properties and outcoupling efficiencies when all active stages are centered within a single antinode of the optical field. The optimized voltage efficiency combined with low optical losses lead to a maximum wall plug efficiency of 0.7%. Flip-chip mounted devices with a 640-$\mu$m squared mesa reached output powers of up to 5.1 mW at ambient temperatures with driving current (voltage) of 0.6 A (5.1 V). © 2019 Society of Photo-Optical Instrumentation Engineers (SPIE) [DOI: 10.1117/1.OE.58.11.117106]

Keywords: interband cascade lasers; mid-infrared lasers; light-emitting devices; absorption spectroscopy; quantum cascade lasers.

Paper 191208 received Sep. 2, 2019; accepted for publication Nov. 13, 2019; published online Nov. 28, 2019.

The growing demand for permanent monitoring of specific molecules in environmental, health, and security applications has created a need for inexpensive and power efficient light sources. In particular, the mid-infrared (MIR) wavelength range from 3 to 6 $\mu$m is of high interest for gas-sensing applications. Compared to the near-infrared spectral region, many technologically and industrially relevant gas species have absorption features with orders of magnitude higher absorbance in this wavelength region.[1] Interband cascade lasers (ICLs) have demonstrated continuous-wave operation at temperatures well above ambient while still keeping low power consumption and are thus well-established light sources in the MIR spectral range.[2]

However, for several applications and spectroscopic techniques, such as methane emission monitoring in agriculture and dairy farming, LEDs represent a broadband, incoherent but cost-effective alternative to lasers.

Without the feedback from an optical cavity, the light emission of the presented interband cascade light-emitting devices (ICLEDs) is not bound to a coherence or gain threshold. Similar to ICLs, the slope efficiency of these devices can be increased by cascading multiple active stages in series, employing the GaSb/InAs broken gap alignment and injector regions to transfer electrons from one emitting stage to the next.

Recent developments show that the efficiency can be further improved by centering the stages of substrate emitting ICLEDs at the antinodes of the near-normal incidence optical field in the vicinity of a metal mirror.[3]

However, due to low outcoupling efficiencies caused by total internal reflection at the high-index substrate to air interface and absorption losses inside the n-doped GaSb substrate, the ICLEDs never exceeded wall plug efficiency (WPE) of 0.4%.[3] The two dominant sub-bandgap absorption mechanisms are free-carrier absorption by free electrons and intervalley conduction-band absorption.

In this work, we present one effective approach to suppress free-electron absorption losses by using low absorbing substrates for substrate emitting ICLEDs.

The nine stage ICLED structure was grown by molecular beam epitaxy (MBE) on low doped GaSb substrates. The MBE system was equipped with valved cracker cells for the group V elements and conventional effusion cells for group III elements and dopants. First, a 500-nm-thick GaSb:Te ($1 \times 10^{18}$ cm$^{-3}$) layer was grown to serve as the contact layer. As shown in Fig. 1, three different configurations were grown, which differ in the arrangement and position of the active stages. While for the first structure, all nine active stages are centered on an antinode of the optical field at normal incidence, the active cores of the second and third structure are partitioned in three groups each made of three active stages. The groups were separated and aligned by GaSb layers so that each group is centered on antinode (node) to meet the condition for constructive (destructive) interference, as shown in Fig. 1 and described in Ref. 3.

Square-shaped ICLED mesa structures with edge lengths of $d = 640$ $\mu$m were wet-etched using a $C_6H_8O_7/H_3PO_4/H_2O_2/H_2O$ solution. To reduce the characteristic current spreading in superlattice-like structures and to improve the performance, the etch was proceeded throughout the active

*Address all correspondence to Nicolas Schäfer, E-mail: nicolas.schaefer@nanoplus.com
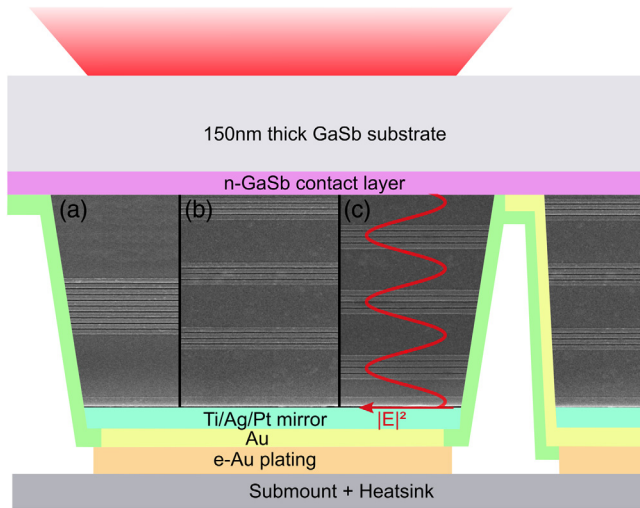
**Fig. 1** Schematic of flip-chip mounted ICLEDs with nine active stages in three different configurations: (a) centered on an antinode, (b) split into three groups positioned at nodes, (c) split into three groups positioned at antinodes of the optical field reflected from the backside metallization.



**Fig. 2** L–I–V characteristics of ICLEDs with mesa edge length of 640 $\mu$m measured in pulsed mode (500-ns pulses, 10-kHz repetition). The nine active stages were positioned in different configurations to investigate the impact of constructive or destructive interference.

region. The etch depth had to be controlled very precisely to hit the position of the 500-nm contact layer, which is located directly underneath the active core. It is crucial to reach an appropriate depth in order to ensure ohmic contacts with low contact resistance. A Ti/Ag/Pt contact metallization was sputtered onto the topside of the mesa, additionally serving as a mirror with a reflectivity of ~94% in the relevant wavelength range. The substrate-side AuGe/Ni/Au contact metallization was sputtered ring-shaped around the mesa and onto a smaller second mesa to level both contacts for flip-chip mounting.

Subsequently, 50 nm of $Si_3N_4$ passivation layer was sputtered by plasma-enhanced physical vapor deposition to prevent short-circuiting the device during the flip-chip mounting, followed by an etch-back using a CHF3-based reactive ion etch process to open contact windows for both substrate and mesa contact. On top of the designated contact areas, 3- to 4-$\mu$m-thick Au layers were electroplated to ensure sufficient heat removal and to serve as mounting bumps.

Due to the absences of a waveguide, the spontaneous emitted light from an LED's active region can be considered internally isotropic. However, only photons propagating within the critical angle for total-internal-reflection $\theta_C$ can outcouple to the outer medium. For commercial LEDs emitting in the visible spectrum, $\theta_C$ is usually defined by the planar interface between the semiconductor and a lens-shaped droplet of epoxy. However, epoxy is not transparent in the MIR and cannot be used, hence, only light directed within a narrow internal cone with $\theta_C \approx 18$ deg given by the high index substrate to air interface can be extracted. The outcoupling efficiency can be improved by either increasing $\theta_C$ (e.g., by means of surface structuring or plasmonic metasurfaces[4,5]) or by redirecting the remainder light into the escape cone. This can be achieved by employing sidewall reflectors, backside structuring, or constructive interference at normal incidence.[6] The latter makes use of the fact that in ICLEDs the photons are generated in precisely located active stages, which can be treated as planes of randomly
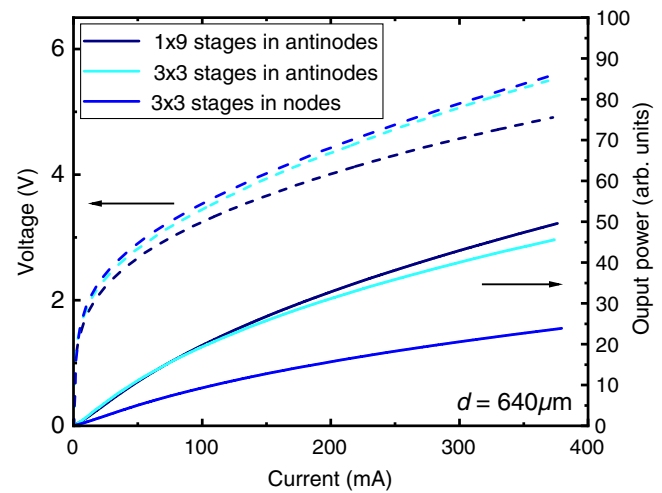
distributed oscillating dipoles. In close vicinity to the metal mirror on the backside (and for light at normal incidence), the upward-radiated electric far field for each dipole arises from interference with the reflected light. At normal incidence, the electric field amplitude $E^2 \propto \cos(2kz)$ forms nodes and antinodes as shown in Fig. 1, with no necessity of a Fabry–Perot cavity. Constructive interference can boost the photon extraction efficiency up to a factor of two compared to uniform stage placement.[6]

Figure 2 presents the L–I–V characteristics of three different ICLED configurations, each with $d = 640$ $\mu$m at ambient temperature, in which constructive (destructive) interference was realized by positioning the active stages in the electric field's antinodes (nodes). The devices were characterized in pulsed mode (500-ns pulses, 10-kHz repetition) on wafer level using a fully automated LED wafer prober. This setup is equipped with a transparent GaAs sample carrier since light is emitted downward through the substrate. Each curve represents the average of 40 to 50 measured devices.

The voltage profile of both stage-separated ($3 \times 3$) ICLEDs is almost identical, which is plausible since the only difference is a change in thickness of the upmost GaSb spacer layer. However, the voltage drop over the ($1 \times 9$) device is considerably smaller since less transition layers between the groups of active stages and GaSb spacer layers with their respective conduction band offset have to be overcome by the carriers.

The output power shows the MIR typical sublinear progression, due to nonradiative Auger recombination, increasing more rapidly with injected carrier density than the radiative rate.[7] At operating currents of 380 mA, the output power for constructive interference is around two-times higher than for destructive interference, even though destructive interference only truly vanishes under ideal conditions, namely monochromatic light, normal incidence and without dispersion as shown in Fig. 3. The cw emission spectra were measured at $T = 20°C$ with injection currents of 200 mA and each spectrum's intensity was adjusted so that its integral corresponds to the total output power of the device. The node
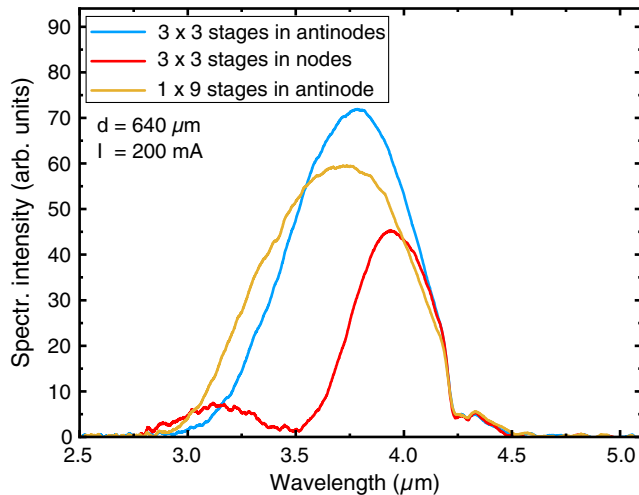
**Fig. 3** cw emission spectra for flip-chip mounted ICLEDs with mesa edge length of 640 $\mu$m at the fixed current of 200 mA. Constructive (destructive) interference at a wavelength of around 3.5 $\mu$m was realized by positioning the active stages in the electric field's antinodes (nodes).



**Fig. 4** Transmission distribution resulting from pulsed optical measurements (500 ns pulses, 10 kHz repetition) of two substrate emitting ICLEDs at fixed currents of 200 and 300 mA. The ICLEDs were grown on low/high doped substrates and were thinned down to various thicknesses.

sample reaches a minimum in spectral intensity for the targeted wavelength of 3.5 $\mu$m. The distortions at 4.3 $\mu$m in all three intensity curves result from $CO_2$ absorption.

Especially, the spectral FWHM of $\sim$700 nm is causing the electric field intensity distribution to smear out, which is why stage groups and spacers should not be too narrow. It must also be noted that the target peak wavelength of 3.5 $\mu$m is slightly off, which affects the correlation between group spacing and peak wavelength. The design with one block of nine stages is spanning a longer distance, making it less susceptible to electric field intensity broadening and deviations from the targeted wavelength, resulting in the highest output power.

Apart from reflection losses, one of the main limitations for extracting the generated photons from substrate emitting ICLEDs is the absorption in the highly Te doped GaSb substrate. The free-carrier absorption by electrons is one of the dominating (optical) sub-bandgap absorption mechanisms at room temperature and prevents the generated photons from reaching the substrate-to-air interface. Related to gallium vacancies and gallium antisites and irrespective of growth technique and conditions, nominally undoped GaSb is always p-type in nature resulting in a residual carrier concentrations of about $10^{17}$ cm$^{-3}$.[8]

To improve the optical transparency, it is essential to reduce the native acceptors, e.g., by lithium diffusion or by tellurium doping compensation, which was first reported by Milvidskaya et al.[9] The latter technique makes it crucial to grow a highly doped GaSb layer in order to form ohmic contacts at the substrate side of the active region.

To investigate the effects of impurity compensation, two samples with a $3 \times 3$ active stage design were grown. One on an n-type GaSb substrate ($n > 5 \times 10^{17}$/cm$^3$) and one on a low doped substrate that requires the mentioned 500-nm Te-doped interstitial layer for the substrate side contact.

Figure 4 shows a series of pulsed optical measurements of substrate emitting samples that have been thinned down to various thicknesses. The substrates were chemically polished to achieve comparable substrate-air reflectivities.
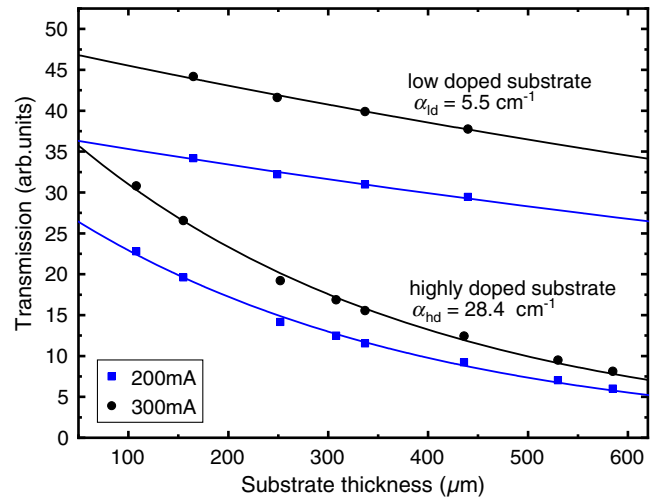
Consequently, the detected output power translates to the transmittance of the substrate. The absorption coefficients of $\alpha = 28.4$ cm$^{-1}$ for the nontransparent and 5.5 cm$^{-1}$ for the semitransparent substrate result directly from the curvature of the transmission distribution. The higher transmittance indicates that an improvement in ICLED light output of 70% is to be expected for the targeted substrate thickness of 150 $\mu$m.

The effective parameters from Ref. 10 are used to calculate carrier concentrations contributing to the absorption mechanisms. For the highly doped substrate, the residual n-type carrier concentration results in $1.3 \times 10^{18}$. The calculation for the semitransparent substrate is more complex since the measurement does not give any information about the carrier type contributing to the absorption. Thus, the effective masses and absorption parameters are bound to have rather large errors associated with it leading to an estimated residual carrier concentration in the $10^{17}$ range.

The most promising stage configuration concerning light outcoupling and electrical properties is the one with a block of nine active stages in an antinode of the optical field as shown in Fig. 2. On this basis, ICLEDs with square-shaped mesa structures ($d = 640 \mu$m) were fabricated and thinned down to 150-$\mu$m thickness using semitransparent GaSb substrates. Single emitters were diced and flip-chip mounted on AlN heat spreaders using AuSn, which were subsequently soldered onto a single layer aluminum PCB. The PCB was attached onto a thermoelectrically cooled measurement station. The devices were analyzed in cw mode concerning their temperature-dependent $L$–$I$–$V$ characteristics and spectral properties (Fig. 5). The total output power was measured using an integrating sphere with a thermoelectric cooled HgCdTe detector. In addition to Auger recombinations, also lattice heating contributes to the $L$–$I$ rollover at high drive currents. The maximum cw output power was $\sim$5.1 mW at $T = 20°$C with a corresponding voltage drop of 5.1 V. Even though no AR coating was used, this result is higher than any previously reported values for MIR LEDs operating at ambient temperature.
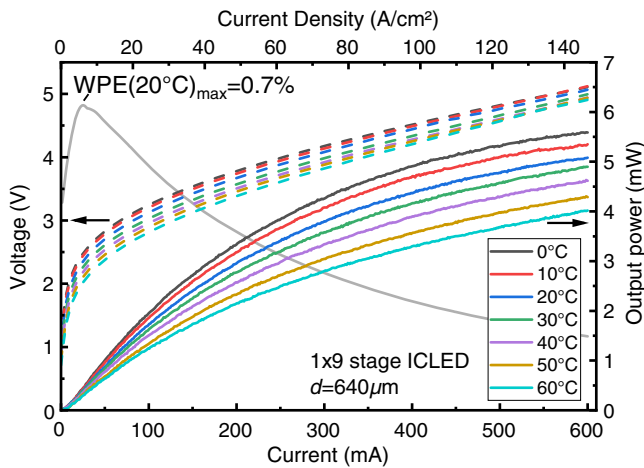
**Fig. 5** cw $L$–$I$–$V$ characteristics for a flip-chip mounted ICLED with $1 \times 9$ active stages and mesa edge length of 640 $\mu$m at seven different temperatures ranging from 0°C to 70°C.

The maximum output power at $T = 20$°C corresponds to an intensity of 1.25 W/cm$^2$, which is less than the reported maximum for smaller, circular-shaped ICLEDs[3] (2.3 W/cm$^2$). This difference can be assigned to the lower number of cascades. Even higher intensities have been reported by Koerperick et al.,[11] although at cryogenic temperatures where radiative lifetimes are decreased and nonradiative lifetimes increased. Figure 5 displays the WPE at $T = 20$°C as function of driving current, which is one of the most important performance indicators for LEDs. The maximum WPE ~0.7% can be achieved at a driving current of 24 mA and a corresponding emittance of 0.1 W/cm$^2$. The WPE ranges from ~0.7% at low powers to ~0.2% at the maximum power. This is two to three times higher than the previous reported values, which were in the range of 0.05% to 0.4%. The improvement in WPE is attributed to the lower doping of the substrate. The great advantage especially at high driving currents is a consequence of the rather large active area, leading to a lower current density of 147 A/cm$^2$ compared to 478 A/cm$^2$ at 600 mA and consequently to less Auger recombinations.

We expect further improvements by enhancing the light outcoupling efficiency through surface texturing such as motheye patterns that broaden the internal cone of the emitted light. Metasurface antennas could also be a suitable candidate since they are not bound to the limitations of total internal reflection, when refracting the emitted light. Moreover, the spatial phase variation enables to effectively control the direction and shape of the refracted wavefront.

In conclusion, ICLEDs were realized that yield higher output powers and WPEs than any previous MIR LEDs operating at ambient temperature. The maximum cw output power when operating at 20°C is 5.1 mW, the WPE ranges from 0.17% to 0.7%. The advantage over previous ICLEDs can be attributed to stage grouping at one single antinode of the optical field and the usage of low absorbing substrates. We expect further improvements by optimizing the GaSb spacer thickness in order to tune the active stages more precisely to the peak wavelength position. The demonstrated

concept is, in principle, compatible to ICLED arrays and efficient emission at longer wavelengths extending into the longwave infrared.

## References

1. L. Dong et al., "Ppb-level formaldehyde detection using a CW room-temperature interband cascade laser and a miniature dense pattern multi-pass gas cell," *Opt. Express* **23**(15), 19821–19830 (2015).
2. I. Vurgaftman et al., "Interband cascade lasers," *J. Phys. D Appl. Phys.* **48**(12), 123001 (2015).
3. C. S. Kim et al., "Improved mid-infrared interband cascade light-emitting devices," *Opt. Eng.* **57**(1), 011002 (2017).
4. C. Luzhou et al., "Simultaneous enhancement of light extraction and spontaneous emission using a partially reflecting metasurface cavity," *Phys. Rev. A* **95**(5), 053808 (2017).
5. T. N. Danilova et al., "Light-emitting diodes based on GaSb alloys for the 1.6-4.4 $\mu$m mid-infrared spectral range," *Semiconductors* **39**(11), 1235–1266 (2005).
6. H. Benisty, H. De Neve, and C. Weisbuch, "Impact of planar micro-cavity effects on light extraction-part I: basic concepts and analytical trends," *IEEE J. Quantum Electron.* **34**(9), 1612–1631 (1998).
7. I. Vurgaftman et al., "Rebalancing of internally generated carriers for mid-infrared interband cascade lasers with very low power consumption," *Nat. Commun.* **2**, 585 (2011).
8. P. S. Dutta, H. L. Bhat, and V. Kumar, "The physics and technology of gallium antimonide: an emerging optoelectronic material," *J. Appl. Phys.* **81**(9), 5821–5870 (1997).
9. A. G. Milvidskaya et al., "The properties of heavily compensated high resistivity GaSb crystals," *Mater. Sci. Eng. B* **22**(2–3), 279–282 (1994).
10. A. Chandola, R. Pino, and P. S. Dutta, "Below bandgap optical absorption in tellurium-doped GaSb," *Semicond. Sci. Technol.* **20**(8), 886–893 (2005).
11. E. J. Koerperick et al., "High-power MWIR cascaded InAs-GaSb super-lattice LEDs," *IEEE J. Quantum Electron.* **45**(7), 849–853 (2009).

**Nicolas Schäfer** received his BS and his MS degree from the Karlsruhe Institute of Technology in 2014 and 2016, respectively, both in physics. He joined the R&D division at nanoplus Nanosystems and Technologies GmbH in 2017, an ISO 9001 and 14001 certified supplier of semiconductor devices and lasers for trace gas sensing. His research interest is in the area of mid-IR light-emitting diodes.

**Julian Scheuermann** received his Dipl Ing degree in nanotechnology engineering from the University of Würzburg, Germany, in 2012. He then joined nanoplus Nanosystems and Technologies GmbH and is now working in the R&D division on advanced laser sources for spectroscopic applications. His research interest is in the area of innovative mid-IR interband cascade-based light sources.

**Robert Weih** received his Dipl Ing degree in nanotechnology engineering and PhD in physics from the University of Würzburg in 2011 and 2018, respectively. In 2015, he joined the epitaxy division at nanoplus Nanosystems and Technologies GmbH, an ISO 9001 and 14001 certified supplier of semiconductor devices and lasers for trace gas sensing. His research interests are in the area of molecular beam epitaxy for innovative mid-IR laser and detector structures.

**Johannes Koeth** received his Dipl phys and PhD from the University of Würzburg in 1996 and 2002, respectively, all in physics. In 1998, he cofounded nanoplus Nanosystems and Technologies GmbH and has been the CEO of the company ever since. His research interests have been in the area of molecular beam epitaxy and innovative semiconductor laser structures. He authored around 150 publications of innovative semiconductor devices and their applications in sensing.

**Sven Höefling** received his diploma in applied physics from the University of Applied Science Coburg, Germany. In 2003, he joined the Department Technische Physik, University of Würzburg, for his PhD work on single-mode emitting quantum cascade lasers. He has been a professor in physics and holds a personal chair at Würzburg University, and the University of St. Andrews, Scotland, since 2015 and 2013, respectively. His research is concerned with the design, fabrication, and characterization of low-dimensional electronic and photonic structures.